Figure S1. Parameters for a normal allometric scaling $\hat{d}_{P_{sys}} = \alpha \cdot M^{\beta}$ (B, dashed line) of the systolic inner diameter of the ascending thoracic aorta ($d_{P_{sys}}$) with body mass (M) of adult male mice (~17 to 40 g body mass) are estimated through a linear regression on the natural logarithms of the two variables (A, dashed line) from 21 control mice on a similar mixed genetic background (crosses in A and B), as reported in (Bellini et al. 2017). The allometric scaling is then refit accounting for perivascular tethering and anesthesia (C, D), which together cause a 39% decrease in luminal pressure and a 21% decrease in systolic axial stretch (Ferruzzi et al. 2018), to reproduce values of inner diameters close to those measured in vivo in anesthetized mice ($d_{P_{sys,adj}}$). The shaded areas envelope 95% confidence intervals. Finally, note that allometric scaling over all ages from birth through adulthood would be expected to result in different values for $\alpha > 0$ and $\beta < 1$, but scaling for these adult male mice is most appropriate herein and the data are described well by this relation.

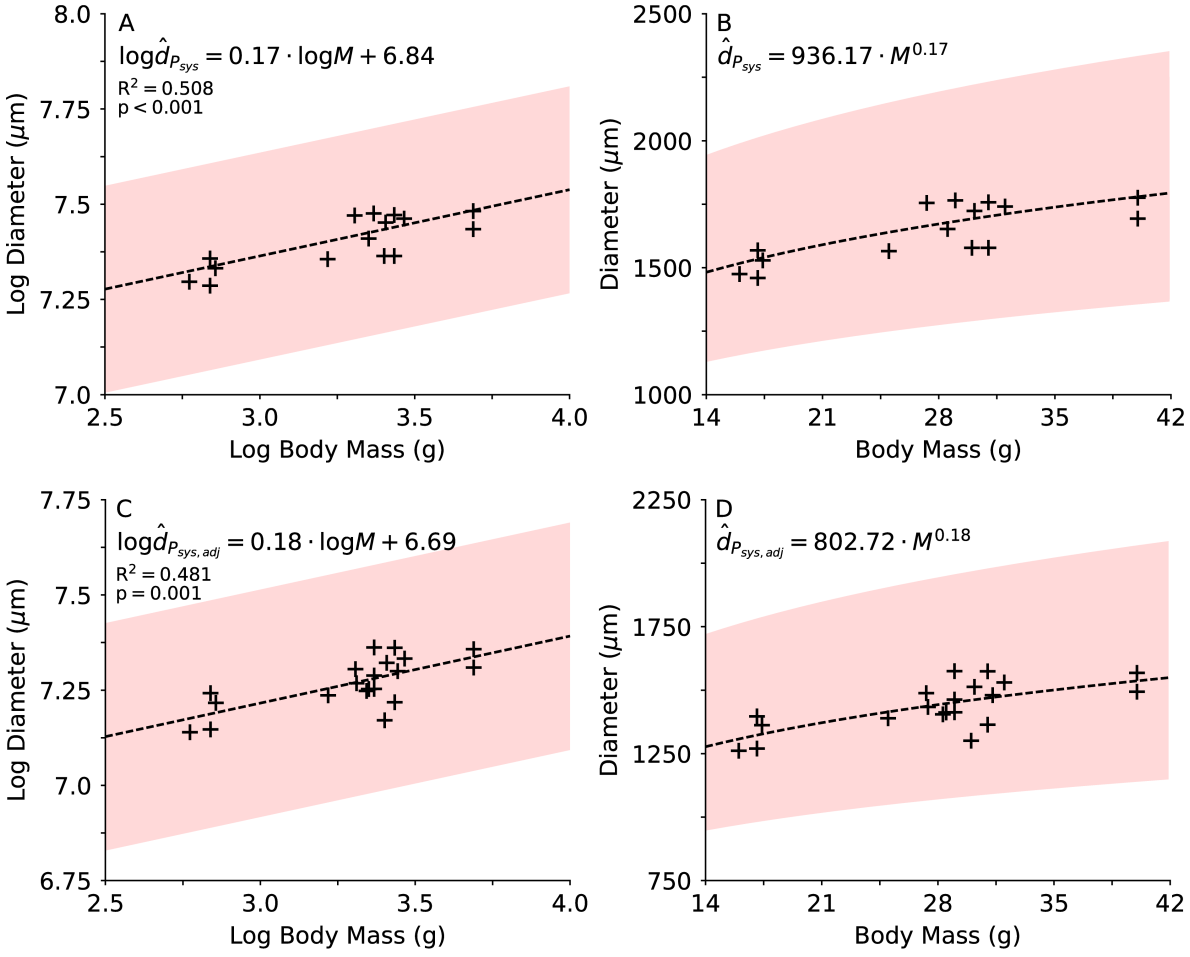

Figure S2. Similar to Figure S1, parameters for a normal allometric scaling $\hat{d}_{P_0} = \alpha \cdot M^{\beta}$ (B, gray dashed line) of the unloaded inner diameter of the ascending thoracic aorta (d_{P_0}) with body mass (M) of adult male mice (~17 to 40 g body mass) are estimated through a linear regression on the natural logarithms of the two variables (A, gray dashed line) from 21 control mice on a similar mixed genetic background (gray crosses in A and B), as reported in (Bellini et al. 2017). Similar to panel K in Figure 1, the estimated allometric relation predicts theoretical changes in the ratio $\hat{d}_{P_0}/M$ as a function of M (C, gray dashed line). In addition, this figure also compares $\log d_{P_0}$ (A), d_{P_0} (B), and ratio d_{P_0}/M (C) for each of the experimental specimens and prior controls (gray crosses, from (Bellini et al. 2017)) to the theoretical curves. Similar to panel L in Figure 1, dot plots of the ratio $d_{P_0}/\hat{d}_{P_0}$ measure how closely each specimen adheres to normal allometric scaling (D). Unlike *Fbn1*$^{\mathrm{mgR/mgR}}$ TAA specimens, double mutant specimens fall within the 95% confidence intervals (shaded areas), confirming that absence of LTBP-3 attenuates the aneurysmal dilatation in the mgR mutant mouse, consistent with its normalization of gene expression, TGFβ signaling, and microstructure (Zilberberg et al. 2015). Statistical significance is set to *p < 0.05.

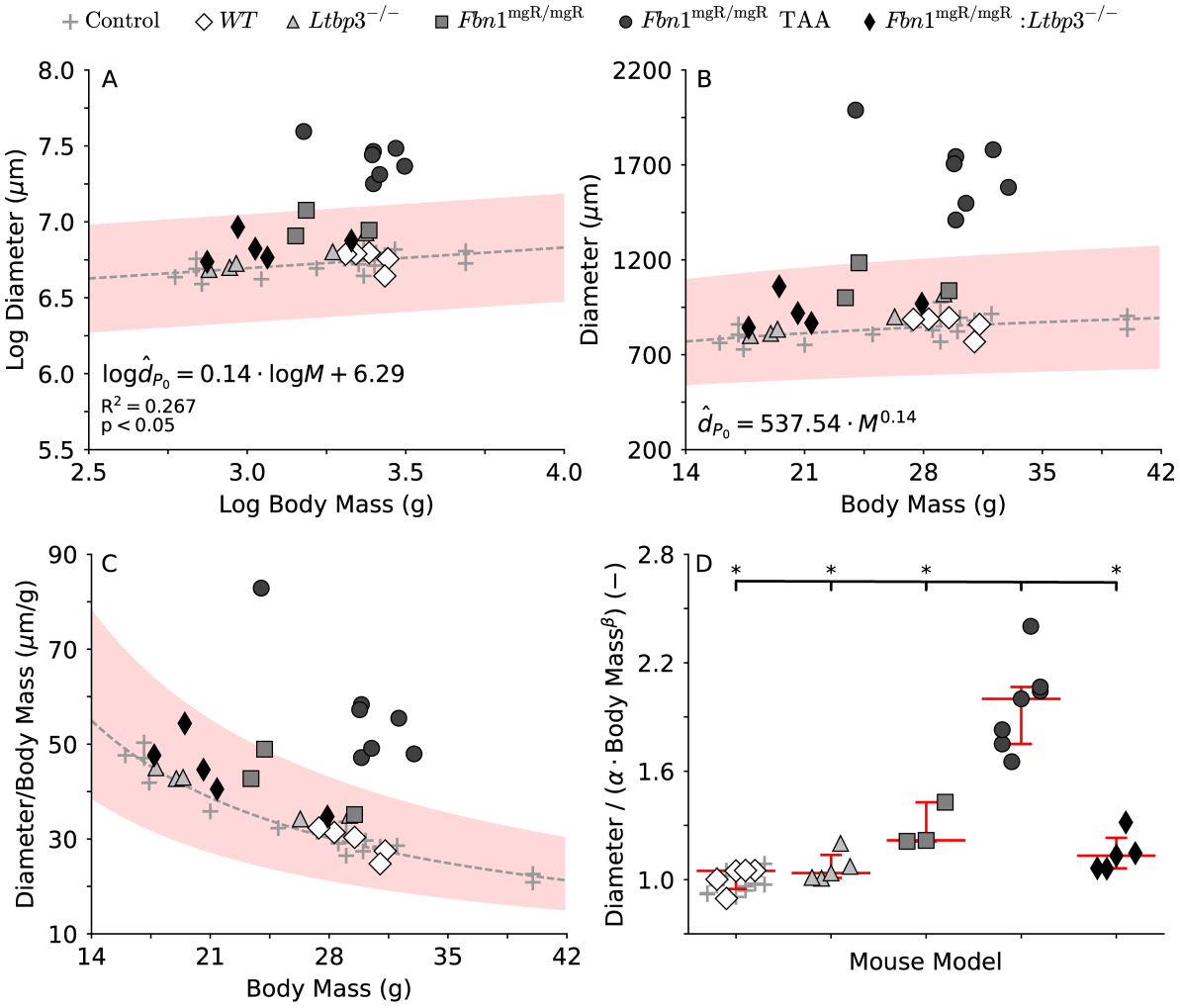

Figure S3. Isoenergy contour plots for the ATA (top row) and the DTA (bottom row) for all four genotypes, with that for the WT shown equally in all plots as light grey curves to facilitate comparisons to controls. Each line identifies combinations of circumferential and axial stretches that result in the same value of stored energy. The symbols (open diamond for wild-type, black circle for the mutants) represent energy storage at 100 mmHg and the group-specific physiologic value of axial stretch, and correspond to the values reported in Tables S1 and S2. Note that adjacent contours radiating outward represent energy values of: 0.1, 1, 5, 10, 20, 40, 60, 100, 250, and 500 kPa, which are thus not incremented equally.

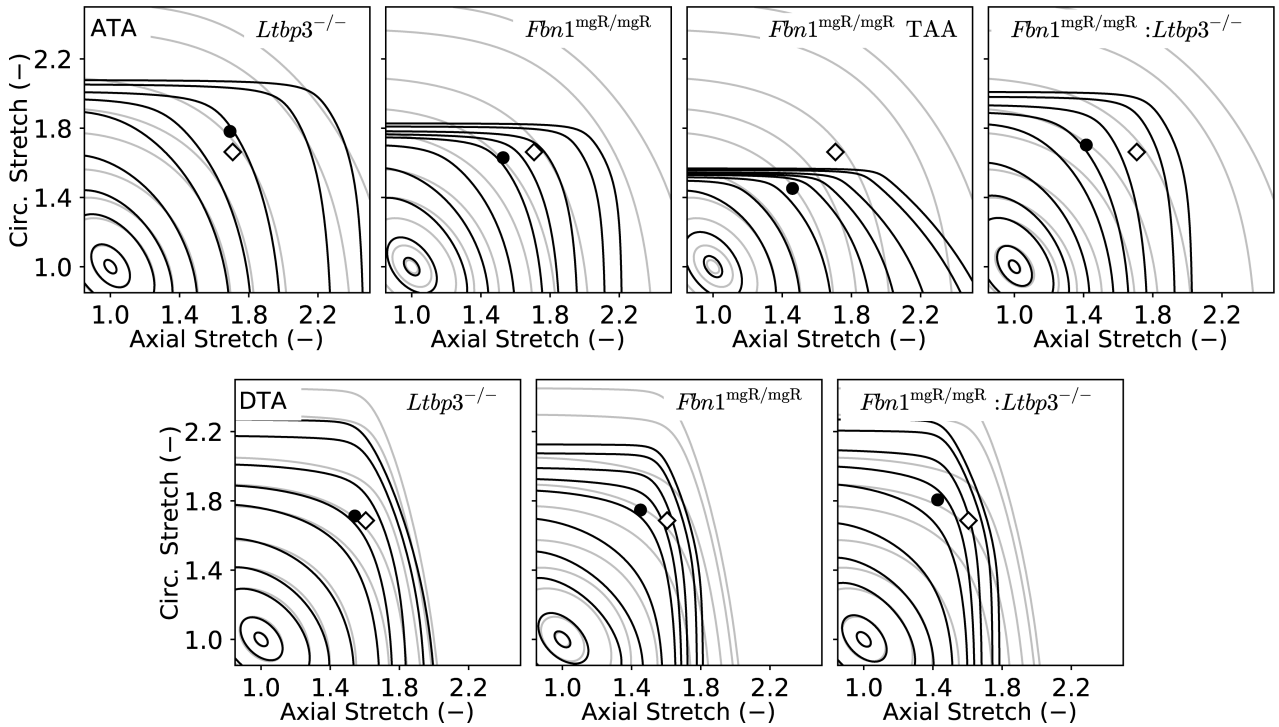

Table S1. Passive geometric, material, and structural metrics of ATAs from all four genotypes: wild-type control (*WT*), LTBP-3 null (*Ltbp3*$^{-/-}$), fibrillin-1 deficient (*Fbn1*$^{mgR/mgR}$) without or with aneurysm (TAA), and double mutant (*Fbn1*$^{mgR/mgR}$:*Ltbp3*$^{-/-}$). Pressure-dependent metrics are calculated at specimen-specific values of in vivo axial stretch but at common pressures of 100 mmHg and 120 mmHg to facilitate comparisons. Superscripts indicate a statistically significant difference, with $p<0.05$ compared to *WT* (*) or *Fbn1*$^{mgR/mgR}$ (†).

	WT	***Ltbp3*$^{-/-}$**	***Fbn1*$^{mgR/mgR}$**	***Fbn1*$^{mgR/mgR}$ *TAA***	***Fbn1*$^{mgR/mgR}$: *Ltbp3*$^{-/-}$**
n	5	5	3	7	5
Unloaded					
Outer Diameter (μm)	1100 ± 38	1095 ± 43	1312 ± 54	1940 ± 75*†	1154 ± 37
Wall Thickness (μm)	112 ± 4	111 ± 3	119 ± 2	134 ± 10	111 ± 3
Inner Radius (μm)	438 ± 17	437 ± 20	537 ± 28	836 ± 37*†	466 ± 19
Axial Length (mm)	2.45 ± 0.12	2.77 ± 0.14	3.91 ± 0.32*	3.92 ± 0.36*	3.09 ± 0.13
Loaded to P = 100 mmHg					
Outer Diameter (μm)	1679 ± 17	1781 ± 64	1998 ± 48	2727 ± 78*†	1814 ± 69
Wall Thickness (μm)	40 ± 3	37 ± 1	48 ± 2	64 ± 3*†	46 ± 2
Inner Radius (μm)	800 ± 8	854 ± 31	951 ± 25	1300 ± 38*†	860 ± 35
Circ. Stretch	1.67 ± 0.05	1.77 ± 0.03	1.64 ± 0.03	1.48 ± 0.03*	1.69 ± 0.02
Axial Stretch	1.70 ± 0.04	1.69 ± 0.05	1.52 ± 0.05	1.42 ± 0.06*	1.41 ± 0.02*
Cauchy Stress (kPa)					
Circumferential	271 ± 19	308 ± 7	266 ± 15	274 ± 11	249 ± 16
Axial	345 ± 31	372 ± 12†	239 ± 18*	196 ± 14*	254 ± 14*
Shear	37 ± 8	32 ± 5	13 ± 6	39 ± 6	9 ± 4*
Linearized Stiffness (MPa)					
Circumferential	1.43 ± 0.09	2.02 ± 0.14†	3.64 ± 0.30*	5.19 ± 0.38*†	1.71 ± 0.19
Axial	1.88 ± 0.16	2.16 ± 0.08	1.65 ± 0.19	1.49 ± 0.15	1.64 ± 0.07
Stored Energy (kPa)	99 ± 10	107 ± 4†	53 ± 4*	39 ± 2*	68 ± 5*
Loaded to P = 120 mmHg					
Outer Diameter (μm)	1766 ± 22	1844 ± 61	2024 ± 47	2751 ± 79*†	1871 ± 70
Wall Thickness (μm)	38 ± 3	36 ± 1	47 ± 2	63 ± 3*†	45 ± 1
Inner Radius (μm)	845 ± 11	887 ± 30	965 ± 24	1313 ± 39*†	890 ± 36
Circ. Stretch	1.76 ± 0.06	1.84 ± 0.03	1.66 ± 0.04	1.49 ± 0.03*	1.75 ± 0.03
Axial Stretch	1.70 ± 0.04	1.69 ± 0.05	1.52 ± 0.05	1.42 ± 0.06*	1.41 ± 0.02*
Cauchy Stress (kPa)					
Circumferential	363 ± 26	398 ± 7	327 ± 18	336 ± 14	319 ± 20
Axial	387 ± 34	408 ± 12†	254 ± 20*	211 ± 15*	282 ± 15*
Shear	15 ± 5	8 ± 3	37 ± 7	62 ± 6*	19 ± 6
Linearized Stiffness (MPa)					
Circumferential	2.11 ± 0.13	3.21 ± 0.37†	6.12 ± 0.97*	8.61 ± 0.58*	3.06 ± 0.56
Axial	2.25 ± 0.19	2.52 ± 0.08	1.79 ± 0.23	1.65 ± 0.18	1.90 ± 0.08
Stored Energy (kPa)	115 ± 12	120 ± 4†	57 ± 5*	41 ± 2*	78 ± 6*
Energy Dissipation Ratio (%)	2.05 ± 0.40	1.98 ± 0.47	5.65 ± 0.25	5.43 ± 1.02*	3.48 ± 0.85

Table S2. Passive geometric, material, and structural metrics of DTAs from all four genotypes: wild-type control (*WT*), LTBP-3 null (*Ltbp3*$^{-/-}$), fibrillin-1 deficient (*Fbn1*$^{mgR/mgR}$), and double mutant (*Fbn1*$^{mgR/mgR}$:*Ltbp3*$^{-/-}$). Pressure-dependent metrics are calculated at specimen-specific values of in vivo axial stretch but at common pressures of 100 mmHg and 120 mmHg to facilitate comparisons. Superscripts indicate a statistically significant difference, with $p<0.05$ compared to *WT* (*) or *Fbn1*$^{mgR/mgR}$ (†).

	WT	***Ltbp3*$^{-/-}$**	***Fbn1*$^{mgR/mgR}$**	***Fbn1*$^{mgR/mgR}$*: Ltbp3*$^{-/-}$**
n	5	7	8	6
Unloaded				
Outer Diameter (μm)	902 ± 8	877 ± 21	933 ± 28	806 ± 16†
Wall Thickness (μm)	111 ± 5	98 ± 5	109 ± 8	110 ± 6
Inner Radius (μm)	340 ± 7	341 ± 14	357 ± 13	293 ± 11†
Axial Length (mm)	5.73 ± 0.41	4.95 ± 0.39	6.32 ± 0.45	5.46 ± 0.33
Loaded to P = 100 mmHg				
Outer Diameter (μm)	1362 ± 30	1360 ± 36	1476 ± 38	1287 ± 42†
Wall Thickness (μm)	41 ± 2	38 ± 2	44 ± 4	43 ± 2
Inner Radius (μm)	640 ± 16	643 ± 19	694 ± 20	601 ± 23†
Circ. Stretch	1.67 ± 0.03	1.70 ± 0.03	1.75 ± 0.05	1.79 ± 0.02
Axial Stretch	1.60 ± 0.04	1.54 ± 0.03	1.45 ± 0.03*	1.44 ± 0.03*
Cauchy Stress (kPa)				
Circumferential	207 ± 12	234 ± 18	224 ± 22	192 ± 18
Axial	240 ± 11	234 ± 21	179 ± 16	170 ± 7
Shear	19 ± 6	6 ± 1	25 ± 7	15 ± 6
Linearized Stiffness (MPa)				
Circumferential	1.13 ± 0.09	1.44 ± 0.08†	2.52 ± 0.40*	1.19 ± 0.25†
Axial	2.88 ± 0.18	2.99 ± 0.26	2.76 ± 0.28	2.55 ± 0.22
Stored Energy (kPa)	64 ± 4	67 ± 8†	44 ± 4	50 ± 3
Loaded to P = 120 mmHg				
Outer Diameter (μm)	1430 ± 32	1417 ± 43	1504 ± 38	1343 ± 41†
Wall Thickness (μm)	39 ± 2	36 ± 2	43 ± 4	41 ± 2
Inner Radius (μm)	676 ± 17	672 ± 23	709 ± 20	631 ± 22
Circ. Stretch	1.76 ± 0.04	1.77 ± 0.04	1.78 ± 0.06	1.87 ± 0.02
Axial Stretch	1.60 ± 0.04	1.54 ± 0.03	1.45 ± 0.03*	1.44 ± 0.03*
Cauchy Stress (kPa)				
Circumferential	277 ± 16	307 ± 26	281 ± 27	252 ± 21
Axial	282 ± 15	272 ± 26	202 ± 19	204 ± 9
Shear	14 ± 5	18 ± 2	39 ± 10	24 ± 8
Linearized Stiffness (MPa)				
Circumferential	1.67 ± 0.14	2.15 ± 0.11	3.57 ± 0.57*	1.78 ± 0.36†
Axial	3.90 ± 0.26	3.99 ± 0.38	3.31 ± 0.35	3.57 ± 0.30
Stored Energy (kPa)	76 ± 5	79 ± 10†	50 ± 5	59 ± 3
Energy Dissipation Ratio (%)	3.90 ± 0.20	2.82 ± 0.71†	7.58 ± 0.68*	3.25 ± 0.73†